

# LUMBER DRYING OF *Pinus*: GEOSTATISTICS APPLIED TO DRYING KILNS

*Winicius Augusto Schaeffer*<sup>1</sup>

<https://orcid.org/0000-0003-0080-2276>

*Thiago Campos Monteiro*<sup>2</sup>

<https://orcid.org/0000-0002-3819-7035>\*

*Ricardo Jorge Klitzke*<sup>2</sup>

<https://orcid.org/0000-0001-6839-9415>

*Allan Libanio Pelissari*<sup>3</sup>

<https://orcid.org/0000-0002-0915-0238>

*Claudio Gumane Francisco Juizo*<sup>4</sup>

<https://orcid.org/0000-0002-8552-174X>

*Tarcila Rosa da Silva Lins*<sup>2</sup>

<https://orcid.org/0000-0002-5809-6741>

## ABSTRACT

This study aimed to evaluate the spatial distribution of the air circulation speed and the final moisture content of pine lumber after kiln drying by using geostatistics. Two kilns acting on boards of 27 mm and 42 mm were evaluated. Air circulation speed and final moisture content were collected in different regions of the kilns. There was no significant difference for air circulation speed and final moisture content between the front and rear regions of the equipment. In the horizontal axis (Y-axis), air circulation speed averages did not differ statistically in both situations, but higher values for this variable were obtained from the spaces between the piles. Final moisture content tended to increase when closer to the door opening. In the vertical axis (Z-axis), the lower part tended to reach higher air circulation speed values. Thus, the spatial behavior influences the air circulation speed and final moisture content during lumber drying. Besides, the variograms presented the same tendency in comparison to the data obtained in a conventional manner, which indicates that geostatistics can be used to represent variables in kilns during the drying process.

**Keywords:** Air circulation speed, moisture content, *Pinus spp.*, spatial behavior, wood drying.

<sup>1</sup>Production manager. Madem Gulf Bahrain. Askar, Kingdom of Bahrain.

<sup>2</sup>Federal University of Paraná. Department of Forest Engineering and Technology. Curitiba, Brazil.

<sup>3</sup>Federal University of Paraná. Department of Forest Science. Curitiba, Brazil.

<sup>4</sup>Instituto Superior Politécnico de Manica (ISPM). Chimoio, Mozambique.

\*Corresponding author: [thiago.monteiro@ufpr.br](mailto:thiago.monteiro@ufpr.br)

Received: 04.12.2020 Accepted: 30.01.2022

## INTRODUCTION

The *Pinus* genus represents 20 % of the planted forests in Brazil (IBÁ 2019). It is the main supplier of sawn wood in the country, and its production exceeded eight million m<sup>3</sup> in 2019 (FAO 2020). Its lumber is mainly destined for the furniture and frame industry, which requires drying processes. Thus, the industrial drying of sawn wood is one of the most important stages of primary wood processing (Ananias *et al.* 2012, Batista *et al.* 2016). Removing water from wood increases its mechanical strength, decreases its mass, facilitates machining, and minimizes the attack of fungi (Kollmann and Côté Jr. 1968).

The wood drying quality depends on numerous factors, such as variations in the final moisture content inside and between boards, residual drying stresses, deformations, collapse in cell walls, and internal or external disruption of tissues, manifested as cracks and splits (Redman *et al.* 2016). It can be controlled based on the technological properties of the raw material, such as density, anatomy, and permeability. In addition, process variables interfere with the drying quality, such as air circulation speed, temperature, and relative humidity inside the equipment. These factors maintain the balance between the rates of surface evaporation and loss of internal water, reducing defects in drying and conducting the process in an economically viable time. Besides, correct drying of pine wood can reduce between 14 % and 35 % of the consumption of heat and electricity in industrial drying (Ananias *et al.* 2012).

Monitoring and control of wood drying can occur in real time using software and sensors. In the last decades, this kind of control has been widely applied in conventional drying. It is performed through programmable logic controllers (PLC), in which variables such as temperature, relative humidity, and circulation speed can be controlled through a computerized interface, allowing manual or automatic adjustment of the drying environment conditions (Bond and Espinoza 2016). However, using these data is still restricted to controlling drying steps and monitoring variables in a few sample points. Thus, there is an exploitable gap for improvement, facing the Industry 4.0 concept and the demands for constant process optimization.

Spatial phenomenon analyses are commonly used in studies on forest management (Pelissari *et al.* 2013, Pelissari *et al.* 2017, Costa *et al.* 2020), technological properties of wood (Lima *et al.* 2006, Carmo *et al.* 2010), and variation of moisture content in chip piles (Valentim *et al.* 2019). However, there is still a wide range of applications in the timber industry, mainly for drying technology. Research on the spatial variation of kiln variables can bring to light methods capable of generating reliable and sufficient data, to the point of promoting robust simulations of spatial behavior, such as “Digital Twins” (Reitz *et al.* 2019), which may provide real-time responses on particularities of the drying process. Thus, this study aimed to evaluate the spatial distribution of the air circulation speed (ACS) and the final moisture content (FMC) of pine lumbers after kiln drying using the geostatistical method.

## MATERIAL AND METHODS

### Lumber drying process

Two conventional drying kilns with a capacity for 80 m<sup>3</sup> and 100 m<sup>3</sup> of lumber were used to dry *Pinus spp.* with thicknesses of 27 mm and 42 mm, respectively. They were located at the company *Moldurarte*, in the municipality of Braço do Norte, State of Santa Catarina, Brazil. They are characterized as side loading - in which woodpiles are moved using forklifts. Both of them had forced convection airflow systems with reversible fans and were subjected to the same sampling method. The lumber dried in this study was employed in the framing industry.

### Spatial location and sampling

The air circulation speed (ACS) and the final moisture content (FMC) of the lumber were evaluated in the drying kilns. Samples for both variables were systematically collected and categorized according to their location in order to obtain the corresponding behaviors considering their origin places. To facilitate understanding, groups of samples were generated for analysis. Each kiln contained 45 piles of boards organized in coordinates in the “XYZ” format - in which “X” represents the pile insertion depth in the kiln (three piles); “Y” represents the lateral distribution of piles (five piles), considering the frontal observation of the kiln with open doors; and “Z” indicates the pile height (three layers). “X”, “Y”, and “Z” coordinates were determined, respectively, from the lower right vertex of the kiln front (Figure 1).

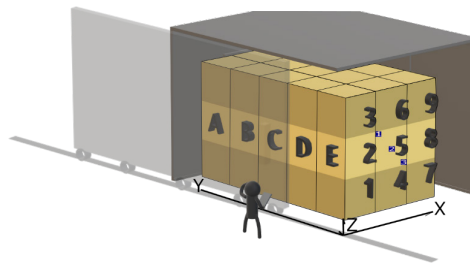


**Figure 1:** Representation of the sampling used to measure the moisture content and air circulation speed of pine lumber in the different regions of the kiln. Where: X = 1 to 9: axis used to evaluate the effect of the pile depth; Y = A to E: axis used to evaluate the effect of laterality in the kiln; Z = 1 to 3: axis used to evaluate the effect of the lumber insertion height; Avatar = view of the results display.

### Obtaining the data

Air circulation speed (ACS) was collected during lumber drying, with the equipment in operation. The kilns in this study have fans that can reverse the airflow during the drying process, which allowed data collection in two moments: first on the front face of the equipment (smaller “X”), followed by the reversal of the airflow and new collection on the rear face of the equipment (bigger “X”). Data were collected using a precision digital thermo-anemometer ( $0,1 \text{ m}\cdot\text{s}^{-1}$ ). ACS was collected inside each pile, between the boards, and outside the piles, between the gaps across the entire drying chamber. The measurements provided 145 values for each face (bigger and smaller “X”). Based on these data, the average ACS behavior in the kiln was obtained.

After drying, three boards were removed from each pile with the aid of a forklift in order to determine the final moisture content (FMC). The pieces were removed at the base, middle, and top of the pile, diagonally, according to the diagram in pile 5E of Figure 1. For each board, two samples of 5 cm each were removed, discarding 30 cm of the top, according to the methodology described by Wallis (1970). In total, 270 samples were obtained from each kiln. The samples were identified, stored in plastic bags, and transported to the Wood Drying Laboratory at the Federal University of Paraná, Curitiba, State of Paraná, Brazil. The mass of the samples was obtained using a digital electronic scale with a precision of 0,01 g. After weighing, the samples were dried in a kiln at  $103 \text{ }^\circ\text{C} \pm 2 \text{ }^\circ\text{C}$  until reaching constant mass. Then, the wood moisture content was determined based on the standard procedure in ASTM D4442 (2007).

The average FMC of two samples represented the average value for each board. The average FMC of three boards represented the average value for each pile. In order to verify more specifically the influence of spatial position on the FMC, two vertical influence groups were created. The first represented the pile height, resulting in an average value from piles at the same vertical level. The second group represented the average value of boards from different piles, but in the same position, that is, under the same “Z”. These groups were called “piles” and “boards”.

Descriptive analyses were performed for all ACS and FMC values, providing general and local averages. The resulting values were compiled according to their positions in the kiln using X real stats supplement from MS Excel. The comparison and verification of statistical differences between the averages of the different positions were performed using the Tukey test. The graphics for horizontal behavior focused on the influence of the Y-axis, and vertical verification for “X” and “Z” was obtained by complementing the study of Schaeffer *et al.* (2020).

## Spatial modeling of data

To perform spatial modeling, values from the front and rear faces of the equipment were used, aiming to compare responses from the same locations, both for FMC and ACS data. Following this methodology, a regular sampling grid was generated (Figure 2). According to Yamamoto and Landim (2013), this methodology reproduces, in a superior way, the distribution and spatial variability of the variable of interest.

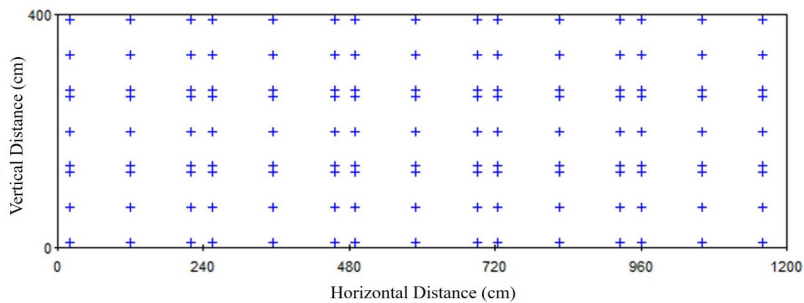


**Figure 2:** Representation of the sampled point grids used in the spatial modeling of air circulation speed (ACS) and final moisture content (FMC) of the boards in the kiln.

Before generating thematic maps, the variogrammetry of the spatial phenomenon was evaluated, which required previous analysis, to verify the nature of the data distribution. If non-normal distributions were verified using the Shapiro-Wilk method, the distribution needed to be normalized, being performed on this volume through weighted log-numeric conversion. The variograms and maps were obtained using the GS + software under different parameters of maximum reach (Active Lag Distance) and steps (Lag Class Distance Interval) in order to return the best model adjustment values while observing the spatial phenomenon. The spherical and Gaussian models were chosen for adjustment.

After adjusting the models, interpolation was performed. The parameter used was point kriging on a uniform grid, looking for pairs in 16 neighbors with a search radius of up to four meters. Axis lines were kept in the thematic maps to represent the spaces between the piles.

## RESULTS AND DISCUSSION

ACS and FMC values of the pine lumber revealed variations between the different heights sampled (Z) and the different regions of the longitudinal axis of the kiln (Y), as presented in Table 1. These parameters showed no difference between the front and rear regions of the drying equipment (X-axis). These results demonstrate tendencies in the behavior of the variables in the kiln.

**Table 1:** Behavior of air circulation speed and final moisture content of pine lumbers with 27 and 42 mm of thickness in the kilns.

Axis	Parameter	Lumber (mm)	Position in the kiln										
			Front			Middle			Rear				
X	ACS (m·s <sup>-1</sup> )	27	3,2 <sup>ns</sup>						3,3 <sup>ns</sup>				
		42	4,7 <sup>ns</sup>						4,2 <sup>ns</sup>				
	MC (%)	27	10,5 <sup>ns</sup>			10,7 <sup>ns</sup>			10,5 <sup>ns</sup>				
		42	13,2 <sup>ns</sup>			13,6 <sup>ns</sup>			13,6 <sup>ns</sup>				
			Walls	A	A-B	B	B-C	C	C-D	D	D-E	E	Walls
Y	ACS (m·s <sup>-1</sup> )	27	4,7 <sup>a</sup> <sub>b</sub>	2,8 <sup>cd</sup> <sub>ef</sub>	3,5 <sup>bcd</sup> <sub>e</sub>	2,7 <sup>defg</sup>	4,3 <sup>a</sup> <sub>bc</sub>	2,8 <sup>cd</sup> <sub>ef</sub>	4,1 <sup>a</sup> <sub>bc</sub>	2,7 <sup>cd</sup> <sub>fg</sub>	3,9 <sup>a</sup> <sub>bc</sub>	2,8 <sup>cd</sup> <sub>ef</sub>	2,0 <sup>f</sup> <sub>eg</sub>
		42	2,1 <sup>c</sup>	3,9 <sup>B</sup>	5,3 <sup>A</sup>	4,1 <sup>B</sup>	5,1 <sup>A</sup>	4,1 <sup>B</sup>	5,4 <sup>A</sup>	4,1 <sup>B</sup>	5,2 <sup>A</sup>	3,9 <sup>B</sup>	3,4 <sup>B</sup>
	MC (%)	27		9,9 <sup>c</sup>		10,1 <sup>c</sup>		10,6 <sup>bc</sup>		10,8 <sup>a</sup> <sub>b</sub>		11,4 <sup>a</sup>	
		42		13,0 <sup>B</sup>		12,8 <sup>B</sup>		13,4 <sup>B</sup>		13,6 <sup>B</sup>		14,5 <sup>A</sup>	
			Base	P1		GS	P2		GS	P3		Top	
Z	ACS (m·s <sup>-1</sup> )	27	5,7 <sup>a</sup>	3,2 <sup>cd</sup>		4,8 <sup>b</sup>	2,6 <sup>de</sup>		2,9 <sup>d</sup>	2,4 <sup>c</sup>		2,9 <sup>d</sup>	
		42	7,6 <sup>A</sup>	3,9 <sup>C</sup>		6,1 <sup>B</sup>	3,8 <sup>C</sup>		5,5 <sup>B</sup>	4,2 <sup>C</sup>		2,9 <sup>D</sup>	
		27		10,4 <sup>b</sup>			10,45 <sup>ab</sup>			10,9 <sup>a</sup>			
		42		13,4 <sup>A</sup>			13,4 <sup>A</sup>			13,5 <sup>A</sup>			

Where: X-axis: used to evaluate the effect of pile depth; Y-axis: used to evaluate the effect of laterality in the kiln;

Z-axis: used to evaluate the effect of the lumber insertion height; For Y: walls; A, B, C, D, and E: location of the pile inside kilns; n-n: space between piles; For Z: Base – the region of the base of lumber piles; P1, P2, and P3: location of piles inside kilns; GS: gap space; Top: region close to the kiln roof. Different letters after the values represent the statistical difference of averages, evaluated by the Tukey test with a 5 % probability. Uppercase letters for boards of 42 mm, and lowercase letters for boards of 27 mm. ns: not significant.

The results in Table 1 demonstrate that in both kilns (with pine boards of 27 mm and 42 mm), ACS and FMC values did not differ significantly between the front and rear regions of the equipment (X-axis). These results may indicate a correct assembly of the drying piles, good storage of the piles inside kilns, and good application of the drying program adopted in the equipment.

In both kilns, ACS averages inside the lumber piles did not vary statistically for the horizontal behavior on the Y-axis (Table 1). The significant differences in these averages are justified by the methodology used since they were compared between the piles, in the empty spaces and close to the walls. ACS values were higher in spaces between lumber piles regardless of the axis analyzed. This behavior was expected and reported in other studies (Vikberg *et al.* 2015). The horizontal air circulation was properly distributed, mainly in the kiln with boards of 42 mm, since it covers all distances related to the walls. This means that the loading and operation of the equipment occurred uniformly.

Deflectors (also known as fins) are commonly found inside conventional kilns, installed on the ceiling and walls, to reduce empty spaces between equipment edges and wood loads. They are equipped with hinges, allowing a better adjustment after mounting the loads. Thus, by observing the high ACS behavior in the “Wall-Piles A” (Walls-A) position of the kiln acting on pieces of 27 mm, distortions in the air directives can be attributed. However, if the fan speed control is not independent, those close to the walls may have lower speeds due to the interference of air friction with the kiln walls. This assigns one more possible cause to the behavior observed on the Y-axis.

The FMC behavior in the Y-axis presented higher values close to one of the equipment walls (E-piles) for both kilns (Table 1). In the equipment with boards of 27 mm, the three sequential piles (D, C, and B piles) exhibited a reduction in the average FMC, with uniform values. Another reduction in humidity occurred in the last pile (A), close to the wall opposite to the highest value. In the equipment with boards of 42 mm, only the region of position E presented higher values for FMC, and the others displayed statistically equal values.

Based on these results, both kilns showed a decreasing tendency for FMC towards the door opening. This behavior can indicate inefficient insulation in one of the walls, generating local condensation and quickly saturating the nearby air. Besides, it is attributed to the removal of wall moisture by the moving air instead of surface moisture of boards (Jankowsky and Galvão 1985). In order to prove this hypothesis, new subsequent drying behaviors must be analyzed.

According to the data in the vertical axis of the equipment (Z-axis), higher ACS values tend to appear in the rear area of both kilns, in the base region (Table 1). The presence of stickers with greater dimensions can favor the airflow in this position since wind tries to flow through the path with the least resistance - in this case, the empty spaces generated by the parts. Higher ACS values also occurred between the piles (Table 1), mainly at the bottom of the equipment with boards of 27 mm. This result can be attributed to the convective movement of the wind, which is directed straight to the bottom of the equipment after hitting the walls and fins. This phenomenon was verified by Zadin *et al.* (2015) through multiphysical simulations representing the airflow behavior in drying kilns.

ACS averages within the wood loads did not differ statistically in the kiln with boards of 42 mm, as seen for piles 1, 2, and 3 (P1, P2, and P3) in Table 1. On the other hand, the equipment with pieces of 27 mm presented a greater difference for the lower piles. This can result due to the nature of the convective movement, which forces air to the bottom of the equipment, and due to smaller lumber thicknesses, responding to the process conditions with increased sensibility. The second factor also results in larger empty spaces in the equipment, consequently increasing the volume of air in motion, which displaces a bigger air mass, despite presenting less expressive speeds. Therefore, the larger amount of displaced air has an expanded capacity to retain and transport moisture, combining and escalating the effect of convective movement with the more sensitive response of smaller boards.

The FMC of piles with boards of 42 mm followed the same behavior, presenting uniform final humidity between the boards at different heights of the kiln (Table 1). On the other hand, the FMC of piles with boards of 27 mm exhibited lower moisture content for boards at the base and middle of the equipment and higher values for piles at the top. Thinner pieces were more sensitive to storage height during the drying process since they differ significantly for the top and the bottom. This behavior can indicate incorrect dimensioning of the equipment or its heating, ventilation, or humidification systems. It can also indicate malfunction of any component or even inconsistencies in the load composition of the woodpiles.

The results for ACS and FMC of the pine piles in the different axes (Table 1) allowed generating graphs for these parameters using the geostatistics method. The variograms allowed the conduction of point kriging, resulting in distribution maps of the variables. The thematic map for ACS inside the kiln with boards of 27 mm can be seen in Figure 3.



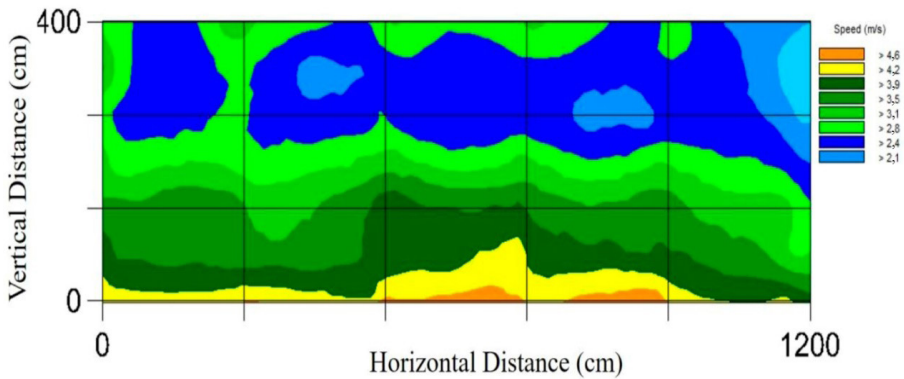


**Figure 3:** Behavior of air circulation speed in a kiln acting on the drying of pine boards of 27 mm.

ACS values in the kiln with boards of 27 mm were higher in the lower region ( $\sim 4,2 \text{ m}\cdot\text{s}^{-1}$ ), with a gradual increase in speed in homogeneous layers along the Z-axis up to approximately half of the equipment height. In the upper third of the equipment height, a larger vertical band was observed, with speeds predominating between  $2,1$  and  $2,4 \text{ m}\cdot\text{s}^{-1}$ . The behavior at the top region represents the expected result for the entire kiln, with lower values in the middle of the piles since this area has a greater physical impediment and consequently less airflow due to the boards. ACS behavior in boards of 42 mm was different when compared to pieces of 27 mm. The kiln acting on boards of 27 mm presented lower and more homogeneous ACS values on the Y-axis when compared to the kiln with pieces of 42 mm (Figure 4). This occurs due to the drying program used, in which thinner boards are dried under lower speeds. From the operational point of view, this configuration is appropriate since different board thicknesses alter a plethora of process variables, especially drying time (Simpson 1991).

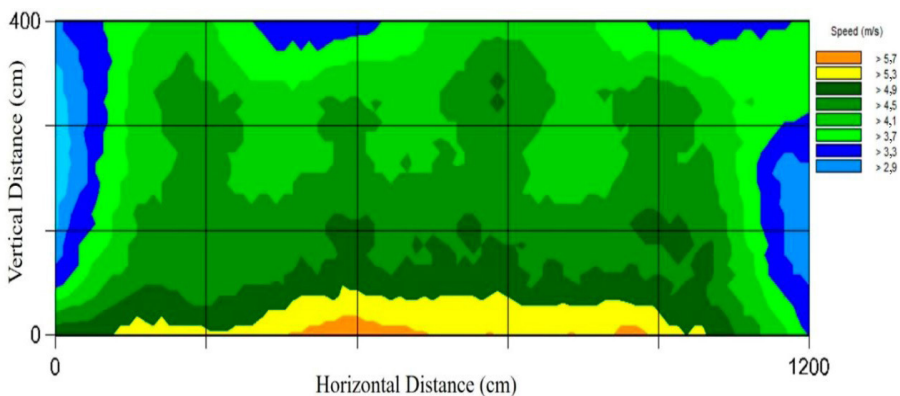


**Figure 4:** Behavior of air circulation speed in a kiln acting on the drying of pine boards of 42 mm.

Higher values for ACS tended to appear in the base-top direction, and lower values on the sides of the kiln (Figure 4), summarizing the results observed in Table 1. The lines on the thematic maps illustrate the empty spaces between the piles. Their lengths and intersections coincide with the regions where high speeds were concentrated. This behavior reinforces the importance of assembling load compositions, which is essential for the uniformity of air circulation speeds (Vikberg *et al.* 2015).

The geostatistics method also allowed visualizing the distribution of the final moisture content in both kilns. Through kriging, a synthesis of Table 1 could be observed once again. FMC values for boards of 27 mm were higher in the horizontal axis (Y-axis), following the door opening direction, and ranged from  $\sim 10,3 \%$  to  $11,6 \%$  (Figure 5). In the vertical axis (Z-axis), the behavior was less clear. Some regions had boards with

low moisture content ( $\sim 10,3\%$ ) and homogeneous distribution along the height, and others showed lower and upper piles with high FMC values when the middle ones presented FMC ranging from  $10,8\%$  to  $11,6\%$ .

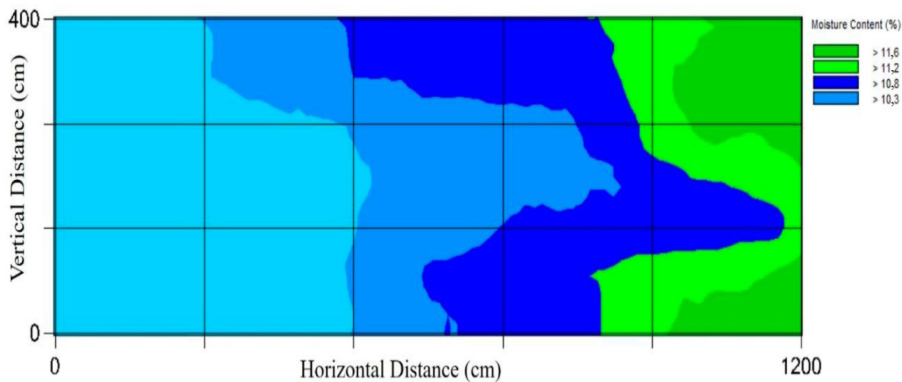


**Figure 5:** Behavior of final moisture contents in a kiln acting on the drying of pine boards of 27 mm.

The FMC behavior was similar for pine boards of 42 mm (Figure 6). However, the horizontal (Y-axis) and vertical (Z-axis) axes presented a greater variation for thicker boards. Once again, the thematic map summarizes the spatial dynamics of the behavior shown in Table 1. Thus, it reiterates the FMC decrease in the opposite direction to the door opening, combined with regions of high humidity ( $\sim 14,7\%$ ).

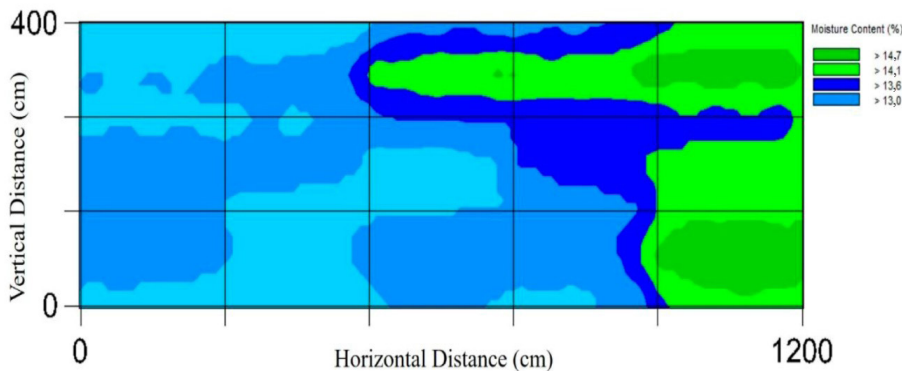


**Figure 6:** Behavior of final moisture contents in a kiln acting on the drying of pine boards of 42 mm.

Overall, the FMC in kilns acting on pine boards of 27 mm and 42 mm (Figure 5 and Figure 6) demonstrates an adequate drying process, requiring only a few adjustments. The variations may occur due to the heterogeneity and complexity of the wood. Radial and tangential boards dry together, as well as boards with different widths. However, wood is an anisotropic material, and its different axes dry differently (Monteiro *et al.* 2020). Besides, variations in board dimensions can affect the drying process (Bramhall 1971), and factors inherent to the drying process can influence the FMC variations. The homogeneous distribution of piles, with low variation in the thickness of the sticks, the correct distribution of humidity sensor pins, among other factors, can cause these variations. It is worth noting that the drying process of both kilns was satisfactory for the processing of wood for the framing industry, with good homogeneity between the FMC values of the boards.

Overall, the problems or inadequacies of the drying process are manifested as defects or inappropriate moisture levels for the intended usage of wood. These issues can cause losses in the product value and indicate resource wastage in drying. Therefore, the use of geostatistics can be an important management tool in the timber industry since it is a fast, efficient, and good final quality process based on knowledge of the variables. Controlling the drying process is of critical importance to achieve the highest quality with the lowest cost (Bond and Espinoza 2016). By understanding and controlling the particularities of the processes, it is possible to allocate resources more efficiently.

Therefore, the geostatistical approach allowed visualizing the spatial dynamics of the variables of interest: air circulation speed inside the kiln and final moisture content of boards in the different regions of kilns. Furthermore, the use of more sensors in the equipment and the measurement of MC and ACS at different times of



lumber drying combined with geostatistics can improve the control of the drying process of *Pinus* wood, thus leaving the raw material factor as the main source of variation in the process. Finally, geostatistics integrated with wood drying software can bring the timber industry closer to the Industry 4.0 concept.

## CONCLUSIONS

Based on the results for the final moisture content (FMC) and air circulation speed (ACS) obtained with the drying of pine boards and by comparing the behaviors according to different analysis methods, it can be concluded that:

The air circulation speed (ACS) inside the drying equipment tends to the spatial behavior connected mainly to the vertical axis.

The final moisture content (FMC) of boards tends to the spatial behavior connected mainly to the horizontal axis of the equipment.

The adjusted exponential models provided thematic maps for final moisture levels and air circulation speeds with the same behavior tendencies observed in the graphical analysis.

There were parametric differences for the different board thicknesses, but their spatial behaviors were similar.

Geostatistics can be applied to represent variables in kilns, reducing the need for sampling and contributing to management optimization in the timber industry.

## ACKNOWLEDGMENTS

All the basic data for this analysis were the result of a partnership between the company Moldurartes, the Foundation of Forest Researches of Paraná (FUPEF), and the Federal University of Paraná (UFPR), based on a technical report to evaluate the occurrence of warping in frames (Klitzke *et al.* 2019).

## REFERENCES

**ASTM. 2007.** Standard test methods for direct moisture content measurement of wood and wood-based materials. ASTM. D4442. 2007. ASTM: West Conshohocken, PA, USA. <https://doi.org/10.1520/D4442-07>

**Ananias, R.A.; Ulloa, J.; Elustondo, D.M.; Salinas, C.; Rebolledo, P.; Fuentes, C. 2012.** Energy consumption in industrial drying of radiata pine. *Drying Technol* 30(7): 774–779. <https://doi.org/10.1080/07373937.2012.663029>

**Batista, D.C.; Klitzke, R.J.; Rocha, M.P.; Batista, T.R. 2016.** Ensaio de taxa de secagem e escore de defeitos para a predição da qualidade da secagem convencional da madeira de *Eucalyptus sp.* – parte 2. *Floram* 23(1): 135–141. <https://doi.org/10.1590/2179-8087.046613>

**Bond, B.H.; Espinoza, O. 2016.** A decade of improved lumber drying technology. *Curr For Reports* 2: 106–118. <https://doi.org/10.1007/s40725-016-0034-z>

**Bramhall, G. 1971.** The validity of Darcy's law in the axial penetration of wood. *Wood Sci Technol* 5: 121–134. <https://doi.org/10.1007/BF01134223>

**Carmo, I.E.P.; Monteiro, T.C.; Santos, G.; Lima, J.T. 2010.** Geoestatística para determinação da variabilidade espacial da dureza da madeira de *Hevea brasiliensis* (seringueira). In Proceedings of the XII Encontro Brasileiro em Madeiras e em Estruturas de Madeira (ed). Lavras, Brasil. (In Portuguese)

**Costa, L.R.R.; Dolácio, C.J.F.; Zea-Camaño, J.D.; Oliveira, R.S.; Pelissari, A.L.; Maciel, M.N.M. 2020.** Variabilidad espacial de *Swietenia macrophylla* en sistema agroforestal de la Amazonia brasileña. *Madera y Bosques* 26(1): e2611937. <https://doi.org/10.21829/myb.2020.2611937>

**Food and Agriculture Organization. FAO. 2020.** Food and Agriculture Organization. Forestry Production and Trade. FAOSTAT Stat. Database. <https://www.fao.org/faostat/en/#data/FO/visualize>

**IBÁ. 2019.** Relatório 2019 Indústria Brasileira de Árvores. 80p. São Paulo, Brasil. <https://iba.org/datafiles/publicacoes/relatorios/iba-relatorioanual2019.pdf>

**Jankowsky, I.P.; Galvão, A.P.M. 1985.** *Secagem racional da madeira*. 2° ed. 108p. Editora Nobel SA: São Paulo. Brasil.

**Klitzke, R.J.; Monteiro, T.C.; Juizo, C.F.G.; Zen, L.R. 2019.** Relatório - Avaliação da ocorrência de empenamentos em molduras de pinus. 54p. FUPEF, UFPR: Curitiba, Brasil.

**Kollmann, F.F.P.; Côté Jr. W.A. 1968.** *Principles of wood science and technology*. 1st ed., ISBN: 978-3-642-87930-2, 592p., Springer-Verlag Berlin Heidelberg: Germany. <https://doi.org/10.1007/978-3-642-87928-9>

**Lima, J.S.S.; Silva, J.T.O.; Oliveira, R.B.; Almeida, V.S.; Vanzo, F.L. 2006.** Estudo da viabilidade de métodos geoestatísticos na mensuração da variabilidade espacial da dureza da madeira de paraju (*Manilkara sp*). *Rev Arvore* 30(4): 651-657. <https://doi.org/10.1590/S0100-67622006000400019>

**Monteiro, T.C.; Lima, J.T.; Silva, J.M.; Rezende, R.N.; Klitzke, R.J. 2020.** Water flow in different directions in *Corymbia citriodora* wood. *Maderas-Cienc Tecnol* 22(3): 385-394. <https://dx.doi.org/10.4067/S0718-221X2020005000312>

**Pelissari, A.L.; Caldeira, S.F.; Ebling, Â.A.; Behling, A.; Figueiredo Filho, A. 2013.** Modelagem geoestatística da dinâmica e distribuição espacial da área basal em povoamento de teca. *Enciclopédia Biosf* 9: 1454-1464. <https://www.conhecer.org.br/enciclop/2013a/agrarias/modelagem%20geoestatistica.pdf>

**Pelissari, A.L.; Roveda, M.; Caldeira, S.F.; Sanquetta, C.R.; Corte, A.P.D.; Rodrigues, C.K. 2017.** Geostatistical modeling of timber volume spatial variability for *Tectona grandis* l. f. precision forestry. *Cerne* 23(1): 115-122. <https://doi.org/10.1590/01047760201723012291>

**Redman, A.L.; Bailleres, H.; Turner, I.; Perré, P. 2016.** Characterisation of wood-water relationships and transverse anatomy and their relationship to drying degrade. *Wood Sci Technol* 50: 739-757. <https://doi.org/10.1007/s00226-016-0818-0>

**Reitz, J.; Schluse, M.; Roßmann, J. 2019.** Industry 4.0 beyond the factory: an application to forestry. In Proceedings of the Tagungsband des 4. Kongresses Montage Handhabung Industrie roboter. Springer Vieweg: Berlin, Heidelberg, Germany. [https://doi.org/10.1007/978-3-662-59317-2\\_11](https://doi.org/10.1007/978-3-662-59317-2_11)

**Schaeffer, W.A.; Zen, L.R.; Klitzke, R.J.; Monteiro, T.C. 2020.** Distribuição espacial do teor de umidade de tábuas de pinus secas em estufa industrial. *Adv For Sci* 7(1): 855-859. <https://doi.org/10.34062/afs.v7i1.9858>

**Simpson, W.T. 1991.** *Dry kiln operator's manual*. *Agriculture handbook*. 274p. U.S. Department of Agriculture, Forest Service, Forest Products Laboratory: Madison, WI. <https://www.fpl.fs.fed.us/documnts/usda/ah188/ah188.htm>

**Valentim, L.B.; Tomeleri, J.O.P.; Thiersch, C.R., Thiersch, M.F.B.M.; Alesi, L.S.; Varanda, L.D.; Almeida, R.E.P.; Yamaji, F.M.; Pádua, F.A. 2019.** Mapping three-dimensional moisture content of wood chip piles for energy production. *Floram* 26 (2): e20180432. <https://doi.org/10.1590/2179-8087.043218>

**Vikberg, T.; Hägg, L.; Elustondo, D. 2015.** Influence of fan speed on airflow distribution in a batch kiln. *Wood Mater Sci Eng* 10(2): 197-204. <https://doi.org/10.1080/17480272.2014.995703>

**Wallis, N.K. 1970.** *Australian timber handbook*. 407p. Halstead Press: Sydney, Australia. <https://citeseerx.ist.psu.edu/viewdoc/download?doi=10.1.1.459.3037&rep=rep1&type=pdf>

**Yamamoto, J.K.; Landim, P.M.B. 2013.** *Geoestatística: conceitos e aplicações*. 1° ed. 215p. Oficina de textos: São Paulo.

**Zadin, V.; Kasemägi, H.; Valdna, V.; Vigonski, S.; Veske, M.; Aabloo, A. 2015.** Application of multiphysics and multiscale simulations to optimize industrial wood drying kilns. *Appl Math Comput* 267: 465-475. <https://doi.org/10.1016/j.amc.2015.01.104>